Supplementary Information (SI) for Soft Matter.
This journal is © The Royal Society of Chemistry 2026

Supplementary Materials: Hydrodynamic scattering of a neutral squirmer by a near-wall curved obstacle: MPCD simulations and analytical theory

Prashant K Nagar[1], Devandar Chauhan[1], Harsh Pandey*[2, 3], Sujin B Babu†[4], and Kamakshi Pandey‡[1]

[1]Department of Physics, Malaviya National Institute of Technology Jaipur, Rajasthan 302017, India
[2]Department of Biotechnology and Chemical Engineering, Manipal University Jaipur, Rajasthan 303007, India
[3]Centre for Water Research and Sustainable Technologies, Manipal University Jaipur, Rajasthan 303007, India
[4]Out of Equilibrium Group, Department of Physics, Indian Institute of Technology Delhi, New Delhi 110016, India

1 Supplementary Materials I

1.1 Squirmer's flow-field

The fluid flow near the swimmer is complex and depends on the geometry and propulsion mechanism. However, further away from the body, fluid can be described as a multipole expansion of the velocity field produced by the swimmer. Under the far field approximation, a swimmer is described by generic features of low Reynolds number fluid. The flow field produced by the spherical squirmer can be written in terms of fundamental singularities as [1]

$$\begin{aligned}\mathbf{u_s}(\mathbf{r}) = &\frac{8\pi\mu}{3}B_1R_s^3\mathbf{u_{sd}}(\mathbf{r},\mathbf{r_s})\\ &+\frac{8\pi\mu}{2}B_2R_s^2\mathbf{u_{fd}}(\mathbf{r},\mathbf{r_s})+\frac{8\pi\mu}{2}B_2R_s^4\mathbf{u_{sq}}(\mathbf{r},\mathbf{r_s})\end{aligned} \tag{1}$$

Where R_s is the radius of the squirmer, $\mathbf{r_s}$ is the position of the stokeslet, $\mathbf{u_s}$, $\mathbf{u_{fd}}$ and $\mathbf{u_{sd}}$ are stokeslet (force monopole), force dipole, and source dipole. Fig. 1 depicts flow fields of Pusher ($\beta = -5$), Neutral ($\beta = 0$) and Puller ($\beta = 5$) squirmers.

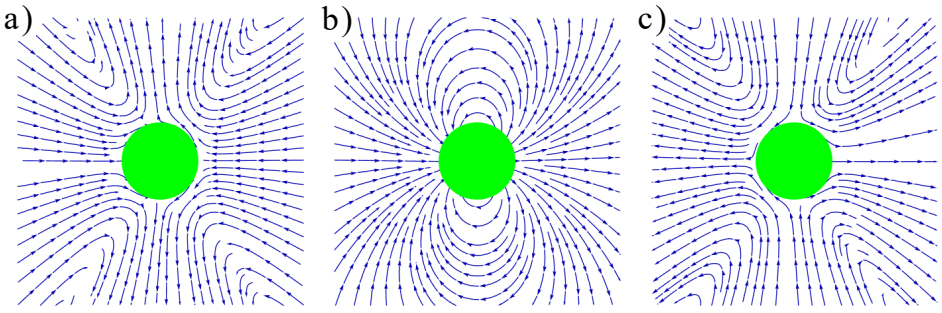

Figure 1: Flow field generated by different types of squirmer a) Neutral ($\beta = 0$) b) Pusher ($\beta = -5$) c) Puller ($\beta = 5$)

*harsh.pandey@jaipur.manipal.edu
†sujin@physics.iitd.ac.in
‡kamakshi.phy@mnit.ac.in

2 Supplementary Materials II

2.1 Accuracy of No-Slip Boundary Condition

The accuracy of the no-slip condition at different portions of the wall is verified by averaging 1000 randomly sampled points. The following tables show the mean for the squirmer at various locations.

$\mathbf{r_s}$	$\mathbf{v_{planar}}$	$\mathbf{v_{circular}}$
(0, 30)	1.253×10^{-4}	1.504×10^{-18}
(0, 50)	2.970×10^{-5}	8.144×10^{-19}
(0, 100)	1.987×10^{-6}	9.355×10^{-21}
(30, 20)	3.624×10^{-5}	5.489×10^{-5}
(30, 50)	6.569×10^{-6}	1.233×10^{-6}
(30, 100)	2.339×10^{-6}	6.681×10^{-9}
(100, 20)	1.189×10^{-6}	3.061×10^{-9}
(100, 50)	3.932×10^{-7}	8.204×10^{-9}
(100, 100)	5.987×10^{-7}	2.318×10^{-9}
(-30, 20)	4.660×10^{-4}	5.863×10^{-5}
(-30, 50)	2.364×10^{-5}	1.300×10^{-6}
(-30, 100)	2.947×10^{-6}	6.894×10^{-9}
(-100, 20)	1.188×10^{-4}	3.287×10^{-9}
(-100, 50)	1.491×10^{-5}	1.797×10^{-7}
(-100, 100)	3.360×10^{-6}	2.300×10^{-9}

Table 1: Mean values of randomly sampled points on the flat and circular portions of the surface, with the squirmer positioned at various locations ($\mathbf{r_s}$). Squirmer radius $R_s = 8a$, Obstacle size $R_o = 16a$, squirmer's orientation $\mathbf{e} = (1, 0)$

$\mathbf{r_s}$	$\mathbf{v_{planar}}$	$\mathbf{v_{circular}}$
(0, 30)	9.951e-05	2.701e-18
(0, 50)	2.312e-05	2.786e-19
(0, 100)	3.037e-06	2.868e-20
(30, 20)	2.867e-04	6.221e-05
(30, 50)	2.015e-05	1.244e-06
(30, 100)	3.504e-06	6.825e-09
(100, 20)	6.912e-05	3.099e-09
(100, 50)	1.018e-05	7.992e-09
(-30, 20)	1.943e-04	5.859e-05
(-30, 50)	1.703e-05	1.240e-06
(-30, 100)	1.920e-06	6.825e-09
(-100, 20)	5.764e-05	7.502e-08
(-100, 50)	9.536e-06	7.968e-09
(-100, 100)	2.455e-06	2.413e-09

Table 2: Mean values of randomly sampled points on the flat and circular portions of the surface, with the squirmer positioned at various locations ($\mathbf{r_s}$). Squirmer radius $R_s = 8a$, Obstacle size $R_o = 16a$, squirmer's orientation $\mathbf{e} = (0.8, 0.6)$

$\mathbf{r_s}$	$\mathbf{v_{planar}}$	$\mathbf{v_{circular}}$
(0, 30)	3.732e-05	4.352e-18
(0, 50)	1.426e-05	4.149e-19
(0, 100)	4.122e-06	4.700e-20
(30, 20)	2.232e-04	5.684e-05
(30, 50)	2.682e-05	1.307e-06
(30, 100)	3.531e-06	6.653e-09
(100, 20)	7.592e-05	3.246e-09
(100, 30)	3.594e-05	5.550e-09
(100, 40)	2.085e-05	7.499e-09
(100, 50)	1.326e-05	7.994e-09
(100, 100)	2.266e-06	2.318e-09
(-30, 20)	2.232e-04	5.467e-05
(-30, 50)	2.682e-05	1.307e-06
(-30, 100)	3.531e-06	6.705e-09
(-100, 20)	7.592e-05	3.138e-09
(-100, 50)	1.326e-05	7.629e-09
(-100, 100)	2.266e-06	2.383e-09

Table 3: Mean values of randomly sampled points on the flat and circular portions of the surface, with the squirmer positioned at various locations ($\mathbf{r_s}$). Squirmer radius $R_s = 8a$, Obstacle size $R_o = 16a$, squirmer's orientation $\mathbf{e} = (0, -1)$

3 Supplementary Materials III

3.1 Scattering trajectory of the neutral squirmer obtained from simulation

The Video S1 depicts the trajectory of a neutral squirmer with radius $8a$ in a channel. The squirmer's initial orientation is aligned with the bottom wall, and it encounters an obstacle of size $16a$ centered in the box. The impact parameter is set to $10a$. The video visualizes the squirmer's motion as it interacts with the obstacle.

4 Supplementary Materials IV

4.1 Trajectories for Varying Obstacle Radii

Scattering trajectories of the neutral squirmer around semicircular obstacles with varying radii are depicted in Fig. 2.

5 Supplementary Materials V

5.1 Scattering trajectory of the neutral squirmer obtained using far-field flow and Faxen's laws

The Video S2 complements Video S1 by demonstrating the calculated trajectory of a neutral squirmer using Faxen's Laws [2, 3]. Faxen's Laws relate the motion of a spherical object to the background fluid flow. Here, we assume a background flow represented by the combination of the three images. The path of the squirmer in Video S1 is recalculated using Faxen's Law for comparison. This video provides a visual representation of the squirmer's trajectory using an analytical approach.

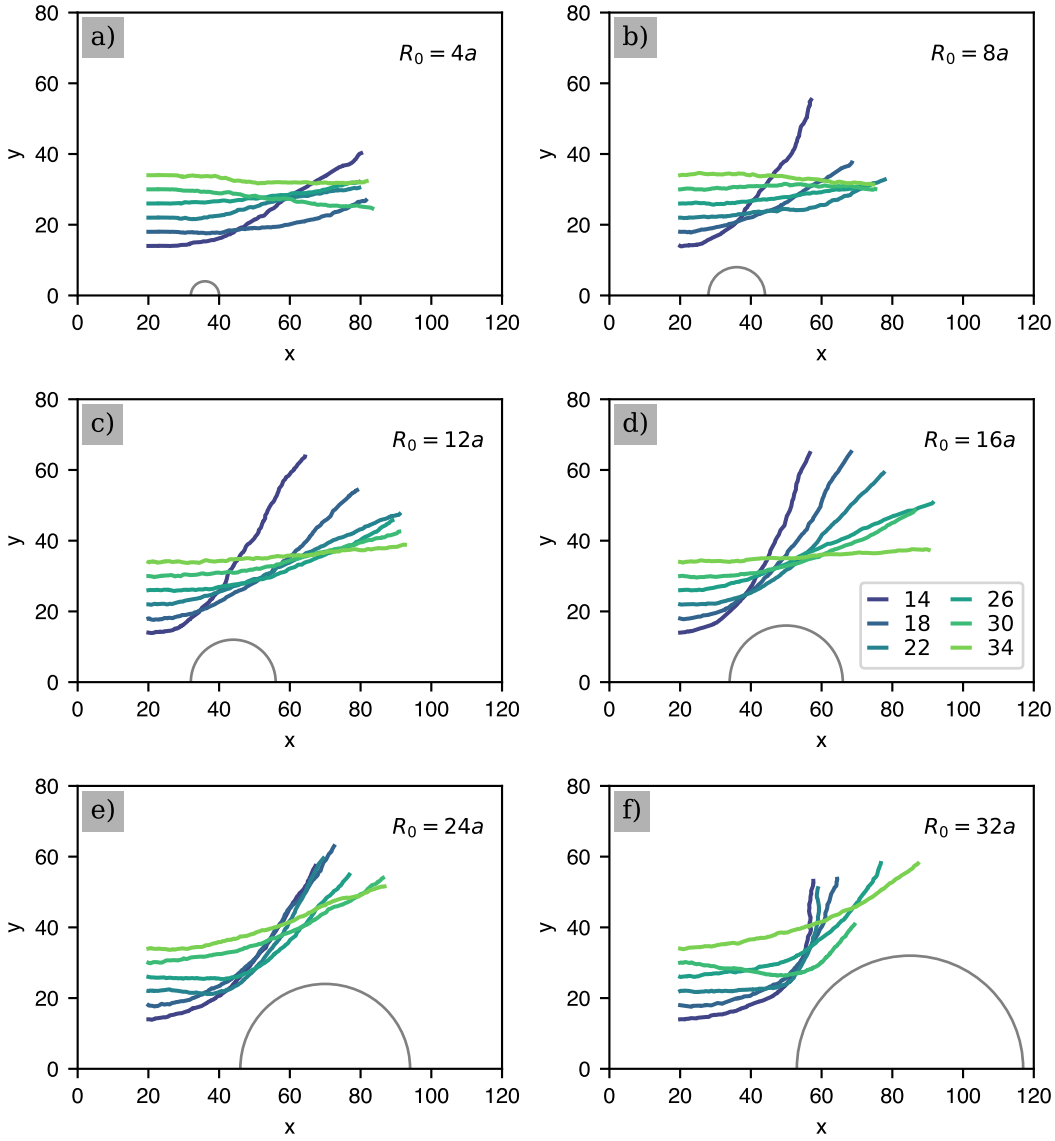

Figure 2: Scattering trajectories of the neutral squirmer ($R_s = 8a$) for different impact parameters h near a semicircular obstacle of varying radius: (a) $R_o = 4a$, (b) $R_o = 8a$, (c) $R_o = 12a$, (d) $R_o = 16a$, (e) $R_o = 24a$, and (f) $R_o = 32a$.

6 Supplementary Materials VI

6.1 Scattering trajectory of the neutral squirmer after including lubrication terms

The Video S3 builds upon Video S2 by incorporating lubrication effects. It presents the squirmer's trajectory in a configuration similar to Video S2, but when the squirmer approaches the obstacle closer than a threshold distance, ε, additional lubrication forces are considered. These lubrication forces are represented by velocity and torque terms added to Faxen's Law calculations. This video shows the squirmer's path when lubrication effects become significant.

7 Supplementary Materials VII

7.1 Scattering from a $1/r^2$ potential

When we assume that the potential energy $V(r) = \frac{k_2}{r^2}$, where k_2 is a positive constant, the $F(r) = \frac{2k}{r^3}\hat{r}$. Here, r is the radial distance of the squirmer from the obstacle. Changing the variable to $u = 1/r$, the equation of the trajectory is given by [4, 5]

$$\frac{d^2u}{d\theta^2} + u\left(1 + \frac{2k_2m}{l^2}\right) = 0 \tag{2}$$

The general solution is given by $U = A\sin(\omega\theta + \beta)$, where

$$\omega = \left(1 + \frac{2k_2m}{l^2}\right). \tag{3}$$

Applying the boundary condition $r \to \infty$, $u \to 0$, thus $\beta = 0$. The distance of closest approach r_{min} is obtained when $\theta = \frac{\pi}{2\omega}$, thus the scattering angle is given by

$$\Theta = \pi\left(1 - \frac{1}{\omega}\right) \tag{4}$$

Substituting eq. 3 in the above equation, we obtain

$$h^2 = \frac{(\pi - \Theta)^2}{\Theta\,(2\pi - \Theta)}\frac{k_2}{E} \tag{5}$$

where $E = \frac{1}{2}mv_0^2$ is the total energy of the system.

8 Supplementary Materials VIII

8.1 Comparison of closest approach $r_{\mathbf{min}}$

The closest approach distance is the minimum distance between the particle and the center of the potential, where the particle's initial kinetic energy is completely converted into potential energy. The analytical formula of $r_{\min}$ for inverse potential is given by

$$r_{\min} = \frac{k_1}{2E}\left(1 + \frac{1}{\sin\left(\frac{\Theta}{2}\right)}\right)$$

and, for the inverse square potential is given by,

$$r_{\min} = \frac{k_2}{2E} + \sqrt{\frac{k_2}{2E} + \frac{k_2}{E}\frac{(\pi - \Theta)^2}{(2\pi - \Theta)\Theta}}$$

This table presents a comparison of the minimum approach distance (r_{min}) between the squirmer and the obstacle (radius $16a$), obtained from simulations and analytical calculations.

Impact	**Simulation**	$\frac{k}{r}$	$\frac{k}{r^2}$
10	25.6685	22.3743	13.4301
12	25.5035	23.9240	15.3595
14	25.3453	25.5701	17.3082
16	25.4823	27.2868	19.2694
18	26.3083	29.0559	21.2391
20	26.4505	30.8647	23.2146
22	27.0125	32.7042	25.1946
24	27.8313	34.5678	27.1779
26	30.5461	36.4506	29.1637
28	30.1752	38.3488	31.1515
30	31.1603	40.2598	33.1409
32	31.5663	42.1812	35.1316
34	33.9653	44.1113	37.1235
36	35.2836	46.0489	39.1162
38	38.3853	47.9928	41.1097
40	41.9147	49.9421	43.1038

Table 4: The closest approach distance (r_{min}) between the squirmer and the obstacle, tabulated for various impact parameters. The values are obtained from both simulation results and analytical formulae based on inverse (k_1/r) and inverse square (k_2/r^2) relationships.

References

[1] M. Kuron, P. Stärk, C. Holm, J. de Graaf, Hydrodynamic Mobility Reversal of Squirmers near Flat and Curved Surfaces, Soft Matter 15 (29) (2019) 5908–5920. arXiv:1904.02630, doi:10.1039/c9sm00692c.

[2] H. Faxén, Der Widerstand gegen die Bewegung einer starren Kugel in einer zähen Flüssigkeit, die zwischen zwei parallelen ebenen Wänden eingeschlossen ist, Annalen der Physik 373 (10) (1922) 89–119. doi:10.1002/andp.19223731003.

[3] J. Happel, H. Brenner, Low Reynolds Number Hydrodynamics: With Special Applications to Particulate Media, Vol. 1 of Mechanics of Fluids and Transport Processes, Springer Netherlands, Dordrecht, 1983. doi:10.1007/978-94-009-8352-6.

[4] H. Goldstein, C. P. Poole, J. L. Safko, Classical Mechanics, 3rd Edition, Addison Wesley, 2008.

[5] R. G. Newton, Scattering Theory of Waves and Particles, Springer Berlin Heidelberg, 1982. doi:10.1007/978-3-642-88128-2.